

# Reactive Surfactants in Heterophase Polymerization. XVII. Influence of the Surfactant on the Mechanical Properties and Hydration of the Films

C. GAUTHIER,<sup>1\*</sup> O. SINDT,<sup>1</sup> G. VIGIER,<sup>1</sup> A. GUYOT,<sup>2</sup> H. A. S. SCHOONBROOD,<sup>3\*</sup> M. UNZUE,<sup>3</sup> J. M. ASUA<sup>3</sup>

<sup>1</sup> G.E.M.P.P.M.–I.N.S.A. Lyon, 20, Av. A. Einstein, 69621 Villeurbanne Cedex, France

<sup>2</sup> L.C.P.P.–C.P.E. Lyon, CNRS UMR 140, 69621 Villeurbanne Cedex, France

<sup>3</sup> Grupo de Ingenieria Quimica, Facultad de Ciencias Quimicas, Universidad del Pais Vasco, Apdo.1072, 20080 San Sebastian, Spain

Received 23 February 2001; accepted 11 September 2001

**ABSTRACT:** In the context of a European union-supported network on “Reactive Surfactants for Heterophase Polymerization,” different polymerizable surfactants (surfiners) have been synthesized and engaged in the emulsion polymerization of styrene, butyl acrylate, and acrylic acid. The thermomechanical properties of films cast from these different latices are reported in this article. The evolution of the mechanical properties with temperature and the effect of water molecules on these properties are studied. We observed that the studied surfactants do not influence the properties of the dry films. However, some differences due to grafting of reactive surfactants appeared when the films were wet. The amount of water uptake is drastically decreased when only reactive surfactants are present in the film. Concerning the mechanical behavior of the wet films, a decrease of the plastic flow stress is observed for all the samples whatever the nature of the surfactant (reactive or conventional). Hence, calorimetric measurements and dynamic mechanical analysis are used to identify the possible mechanisms that induce the change in the mechanical behavior of the latex films. In the case of reactive surfactant grafted to the polymer, the very low value of water uptake is accompanied by a plasticization of the polymer. In contrast, no plasticizing effect is observed in the case of nonreactive surfactant, even if the amount of water is very large. Finally, the tensile behavior of the styrene–butyl acrylate copolymer versus temperature is analyzed in the frame of the quasi point defects (qpd) model. Both rubber elasticity and chain orientation effects are taken into account to describe the behavior laws at large extensions (i.e.,  $\epsilon \approx 1.2$ ). © 2002 Wiley Periodicals, Inc. *J Appl Polym Sci* 84: 1686–1700, 2002; DOI 10.1002/app.10548

**Key words:** latex films; polymerizable surfactants; water uptake; thermomechanical properties

## INTRODUCTION

Surfactants play a crucial role in the production and application of the dispersed polymers. They

are very important for the nucleation of the latex particles, the emulsification of the monomer droplets, and the stabilization of the polymer particles during polymerization and the shelf-life of the products. However, they can have adverse effects because they can cause foaming, and when mixed with other products in paints, the surfactant may migrate to the pigment phase and cause destabilization of the latex particles. There can be further problems during processing of the latex; for example, when the latex is coated at high-application speeds, the surfactant can desorb under the influence of the high shear and cause desta-

---

Correspondence to: C. Gauthier (catherine.gauthier@insa-lyon.fr).

This publication is part of a series of publications from the EU program “Human Capital and Mobility” (CHRX CT 930159) on “Reactive Surfactants for Heterophase Polymerization.”

\* Present address: Wacker Chemicals Australia, 11 Leicester Avenue, Glen Waverley VIC 3150, Australia.

Contract grant sponsor: Rhodia Recherches.

*Journal of Applied Polymer Science*, Vol. 84, 1686–1700 (2002)  
© 2002 Wiley Periodicals, Inc.

bilization. The stability of the latex may also be disturbed by freeze and thaw cycles. Once the latex has been applied in films and coatings, the surfactant can migrate to the film–air surface and affect gloss. It can also migrate to the film–substrate interface reducing adhesion.

A way to reduce the negative effects of the surfactants is to use surfmers. A surfmer is a surfactant molecule that contains a polymerizable double bond. The publications concerning the use of surfmers have been recently reviewed<sup>1</sup> (previous reviews include those given in refs. <sup>2, 3,</sup> and <sup>4</sup>). Cases reported in literature in which the use of surfmer led to improvements in processes and/or products as well as the requirements for the optimal performance of the surfmer were discussed.<sup>5,6,7</sup> Previous studies have proven that the freeze/thaw stability can be improved by use of reactive surfactants. However, these reviews show that there is a lack of information about the effect of the surfmers on the mechanical properties of the films.

The present work deals with the properties of films cast from latices containing polymerizable surfactants. In the context of a European Union-supported network on “Reactive Surfactants for Heterophase Polymerization,” different surfmers have been synthesized, which differ mainly with respect to the nature of the polymerizable moiety. They have been engaged in the emulsion polymerization of the styrene/butyl acrylate/acrylic acid system. The mechanical properties of films cast from the different latices will be studied and compared. The focus will be on the influence of temperature and water uptake on the film properties.

## EXPERIMENTAL

### Latice Synthesis

All the studied latices have been synthesized through radical emulsion polymerization. Two different synthesis routes have been followed. Both of them have been already described in detail in refs. <sup>8</sup> and <sup>9</sup>.

The first route is a two-step polymerization leading to core-shell particles.<sup>8</sup> In a first step, a batch polymerization of styrene was carried out at 70°C to obtain a seed latex. The resulting particle dispersion presented an average diameter of 100 nm. A second polymerization stage was carried out onto this seed by using a semibatch polymerization procedure, with the addition of a mixture of styrene, butyl acrylate, and acid

acrylic (weight ratios are 49, 50, and 1 g per 100 g of polymer, respectively). The final latices consisted of a dispersion of spherical particles (200 nm in diameter) with a very narrow particle size distribution, as measured by dynamic quasi-elastic light scattering.

In the colloid, the particles were stabilized either by the conventional surfactant (sodium dodecyl sulfate, SDS), which is adsorbed and covers the surface, or by grafted surfmers. Two kinds of surfmers were used, as follows:

- a half-ester of maleic anhydride, or monododecyl maleate (HEC<sub>12</sub>);
- the ethoxylated derivative of this monododecyl maleate (C<sub>12</sub>M—OE<sub>45</sub>—CH<sub>3</sub>).

In the following, the first set of samples are identified as OS-latices and called, respectively, SDS, HEC<sub>12</sub>, and C<sub>12</sub>MPOE, referring to the used surfactant. It must be stressed that, in this route, a washing procedure was used, for both HEC<sub>12</sub> and C<sub>12</sub>MPOE, to eliminate the surfactant that was only adsorbed. In that way, the difference in the mechanical behavior of samples with conventional surfactant and surfmers will be due only to the grafted entities' contribution. It may be added that the conversion (or degree of grafting) was found equal to 87% for HEC<sub>12</sub> and 70% for C<sub>12</sub>M—OE<sub>45</sub>—CH<sub>3</sub>. As the washing procedure is time consuming and will not be used in an industrial recipe, this set of samples can be regarded as a model system.

The second route is a semicontinuous polymerization of a terpolymer of styrene/butyl acrylate/acrylic acid, with a composition of 49.5/49.5/1 g per 100 g of polymer.<sup>9</sup> Three latices of this polymer have been stabilized by (1) the conventional SDS surfactant referred to as 55SDS; (2) a maleate sulfonate referred to as 55M141; (3) the homologue crotonate referred to as 55CRO. Thus, physically adsorbed surfactant molecules stabilize the 55SDS latex particles, whereas surfmer molecules stabilize the 55M141 and 55CRO latices. A fraction of them are chemically grafted at the particle surface. Because the grafting of the surfmers was not complete, there is also some nongrafted, but physically adsorbed, reactive surfactant molecules present in these two latices; the conversion (or degree of grafting) of the maleate surfmer in 55M141 was ~ 64% and the conversion of the crotonate surfmer was ~ 15%. For these three latices, the average diameter of particles was around 170 nm, as measured by dy-

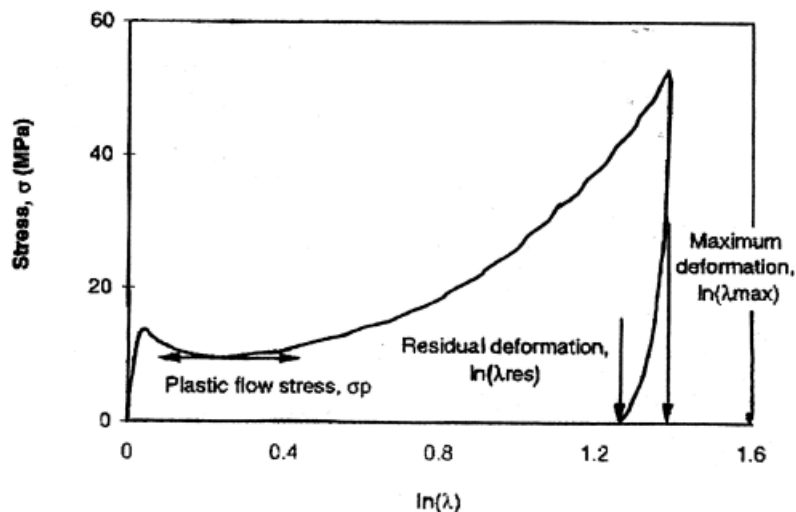


**Figure 1** Tensile behavior of a styrene-butyl acrylate film. Definition of  $\sigma_p$  and  $\lambda_{res}$ .

namic quasi-elastic light scattering. They had a solid content of 26% after dilution (they were prepared at 55% solid content).

This second set of latices will be referred to as MJ-latices. The main difference with the first set of samples is the absence of washing procedure. In other words, the MJ-latices based on surfimers contain both grafted and adsorbed surfactants and can be regarded as a more industrial-like system.

### Film Formation

Before casting the films, the latices were diluted to 10% solid content with some freshly deionized water. Then, each latex was sprayed onto rectangular PTFE molds of  $60 \times 50 \text{ mm}^2$ . The forms were filled with 10 g of the latex and put in an oven that allowed controlling temperature and relative humidity (RH). The temperature was set to  $T = 32 \pm 0.1^\circ\text{C}$  and the RH was maintained at  $75 \pm 2\%$ . The loss of weight was followed versus time until no further significant weight decrease because water evaporation was measured. Then, the samples were aged in the oven (at  $32^\circ\text{C}$  and 75% RH) for at least 2 weeks, to achieve complete macromolecular interdiffusion and then full mechanical properties. This procedure resulted in transparent latex films with a thickness of 0.7 mm.

### Thermomechanical Tests

The tensile tests were performed on an Instron 1026 apparatus. Samples were dumbbell-shaped with typical dimensions of 4 mm width and 25

mm length. Nominal strain  $\epsilon_n$  and nominal stress  $\sigma_n$  are given by the relationships  $\epsilon_n = (L - L_0)/L_0$  and  $\sigma_n = F/S_0$ , where  $F$  is the applied force,  $L$  is the sample length during the test ( $L_0$  at  $t = 0$ ), and  $S_0$  is the initial sample cross section. In the assumption of constant volume, true stress and true strain can be deduced from nominal data by  $\epsilon = \ln(\lambda) = \ln(1 + \epsilon_n)$ , where  $\lambda$  is the stretching ratio ( $\lambda = L/L_0$ ) and  $\sigma = F/S = (1 + \epsilon_n)\sigma_n$ .

The following procedure was adopted: the sample was loaded until the strain  $\epsilon = 1.4$ , which corresponds to an increase of the length ( $L - L_0$ ) of 85 mm. Then, the sample was unloaded until the stress was equal to zero. The crosshead speed was constant and equal to 50 mm/min for both the loading and the unloading paths. The test temperature was varied between 20 and  $70^\circ\text{C}$ , with an accuracy of  $\pm 0.2^\circ$ . This temperature range was chosen because at  $T < 20^\circ\text{C}$ , the samples broke before reaching the desired strain, whereas at  $T > 70^\circ\text{C}$ , the signal displayed by the force sensor was below the sensitivity of the apparatus. Two parameters will be mainly discussed in this article. First, the plastic flow stress ( $\sigma_p$ ) corresponds to the minimum value observed in the stress-strain curve, roughly at a deformation [ $\epsilon = \ln(\lambda)$ ] of around 0.2 (see Fig. 1). When the tensile test is performed at temperatures higher than  $T_g$ , a minimum in the stress-strain curve is hardly observed;  $\sigma_p$  is then determined for  $\epsilon = 0.2$ . The second parameter is the ratio between the residual deformation taken immediately after the unloading and the maximum deformation [ $\ln(\lambda_{res})/\ln(\lambda_{max})$ ]. This ratio ranges from 0 to 1. A value of 1 means that no deformation is recovered; a poly-

mer tested at a temperature well below its main mechanical relaxation transition ( $T_\alpha$ ) may tend to behave similar to this. A value of 0 means that the deformation is fully recovered after the unloading path, just like in the case of a crosslinked polymer in the rubbery state. Several samples (between two and five) have been tested to determine both parameters with a good accuracy. The reproducibility was found to be better than  $\pm 5\%$  for  $\sigma_p$  and  $\pm 2\%$  for the ratio  $[\ln(\lambda_{\text{res}})/\ln(\lambda_{\text{max}})]$ .

To study the water rebound of the different films, parts of fully cured films were dried overnight under vacuum at  $40 \pm 1^\circ\text{C}$ . Then, they either were stored at ambient temperature over some dehydrant (silica-gel) or were immersed in deionized water. The water uptake was allowed to take place for 2 weeks (the temperature and time of water uptake were exactly the same for all the films). Subsequently, the thermal and the mechanical properties of both dry and hydrated films were investigated. In the case of dry and hydrated films, the tensile tests were performed until failure.

Dynamic mechanical analysis was performed by means of a torsion pendulum developed in our laboratory and currently provided by Metravib.<sup>10</sup> Isochronal measurements were carried out on this apparatus at a fixed frequency of 1 Hz and a heating rate of  $1^\circ\text{C}/\text{min}$ . A hydrated sample was cooled from 25 to  $-70^\circ\text{C}$  and then reheated to  $70^\circ\text{C}$  in air. The real part of the complex shear modulus ( $G'$ ) and the loss factor ( $\tan \delta$ ) were measured and plotted versus temperature. The film was subsequently dried under vacuum for 2 h at  $70^\circ\text{C}$ , before cooling to  $-70^\circ\text{C}$ . A last temperature run was performed in a dry helium atmosphere. Under these conditions, the first two scans allow us to determine the properties of a hydrated film during freezing and thawing,

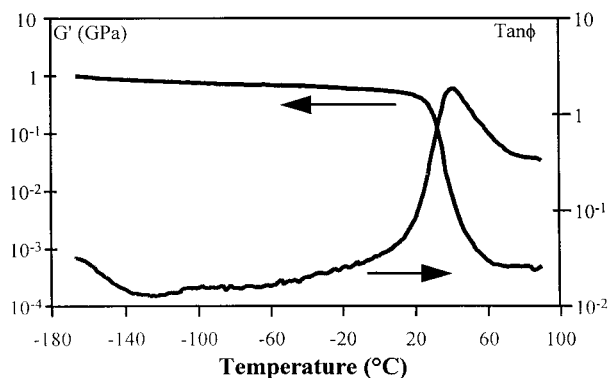


**Figure 2**  $G'$  and  $\tan \phi$  versus temperature at 1 Hz for the film cast from the SDS latex.

**Table I** Characteristics of the Dynamic Mechanical Spectra for the Lattices of the OS Series

	SDS	HeC <sub>12</sub>	C <sub>12</sub> MPOE
$T_\alpha$ ( $^\circ\text{C}$ ) (1 Hz)	40	37	35
$\tan \phi$ max.	1.85	2.05	2.3
$G'_{g(0^\circ\text{C})}/G'_{r(60^\circ\text{C})}$	770	820	880

whereas the last scan concerns the sample in the dry state

## RESULTS

### Model Core-Shell Systems (OS-Series)

#### Mechanical Behaviors of Dry Films

The dynamic mechanical behavior of the samples from the OS-series was investigated at low strain in the linear regime. The evolutions of the real part of the modulus ( $G'$ ) and the loss factor ( $\tan \phi$ ) versus temperature are given in Figure 2 for the SDS film. Spectra recorded for the HeC<sub>12</sub> and C<sub>12</sub>MPOE films are very similar; the temperature of the main relaxation ( $T_\alpha$ ), the maximum value of the loss factor ( $\tan \phi_{\text{max}}$ ), and the drop of modulus between glassy and rubbery plateau ( $G'_{g(0^\circ\text{C})}/G'_{r(60^\circ\text{C})}$ ) are given for comparison in Table I. When the reactive surfactants are used, the modulus in the glassy state is almost unchanged but the characteristics of the  $\alpha$ -relaxation, related to the glass transition of the polymer, are slightly affected. Actually, the use of reactive surfactants induces a decrease of  $T_\alpha$  and an increase of  $\tan \phi_{\text{max}}$ . This evolution may be attributed to a plasticizing effect, probably related to the hydrophilic part of the surfmer. Moreover, as the main relaxation temperature is different from one sample to another, any comparison of the mechanical behavior, especially in the temperature range near  $T_\alpha$ , should be done by using normalized (also called reduced) temperature (i.e.,  $T/T_\alpha$ ).

The stress versus strain curves at different temperatures are given in Figure 3 for the SDS latex film. For  $20^\circ\text{C} < T < 30^\circ\text{C}$ , the tensile behavior of the film shows a viscoplastic behavior, with a hardening at high strains [ $\ln(\lambda) > 0.4$ ]. The behavior changes in the temperature range close to the main relaxation. When the temperature is higher than  $50^\circ\text{C}$ , the latex films behave as a rubberlike material: low stresses are measured and a significant part of the deformation is recov-

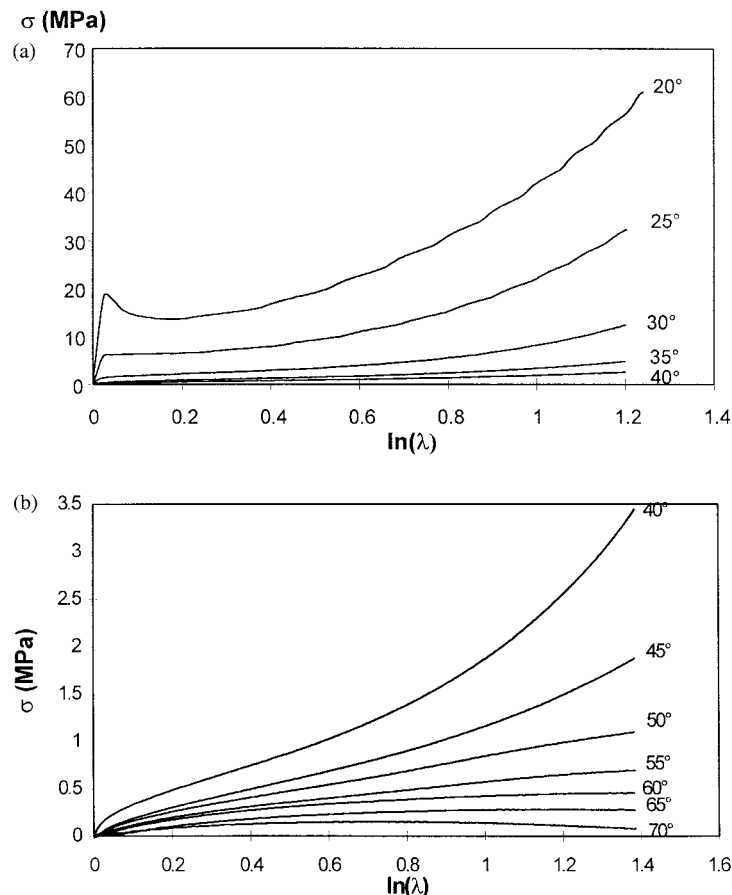


**Figure 3** Evolution of the stress versus strain during tensile tests for the SDS latex, as a function of temperature. (a) Stress/strain curves between 20 and 40°C; (b) stress/strain curves between 40 and 70°C.

ered after unloading. However, even at high temperature, the strain recovery is not complete.

The whole set of stress–strain curves in the case of films based on surfmers displays very similar behavior. To estimate the influence of surfmer on the stress–strain curves, the values of plastic flow stress and of the normalized residual deformation for films formed with SDS and HeC<sub>12</sub> latices have been reported in Figure 4 (data concerning C<sub>12</sub>MPOE are not available on the whole range of temperature). Figure 4(a) is a plot of plastic flow stress versus temperature using a semi-logarithmic scale. Such a representation proves the existence of two domains, in agreement with Figure 3: below  $T_{\alpha}$ , the plastic flow stress decreases sharply with  $T$ , whereas above  $T_{\alpha}$ , the decrease is slowed down. The evolution of the normalized residual strain versus temperature [Fig. 4(b)] also points out two domains. In the low-temperature region, the ratio decreases with the temperature. This is the expected behavior of

a polymer when temperature approaches  $T_{\alpha}$  and even goes through it: the material slowly begins to be rubberlike so the residual deformation is expected to decrease. However, at temperatures higher than  $T_{\alpha}$ , instead of a full recovery of the deformation, the residual deformation increases again with temperature. This can be attributed to the flow of the polymer that may occur because the polymer is not chemically crosslinked. As temperature increases, the flow is more pronounced because the average time associated to the flow of the polymer becomes comparable to the time scale of the experiment and decreases with temperature (i.e., the viscosity decreases for temperatures higher than  $T_g$ ). So, the minimum observed in Figure 4(b) reflects the competition between the rubberlike behavior and the flow of macromolecules. If we compare the results from the point of view of conventional and reactive surfactants, it appears that the data obtained for the SDS films are very similar to the data for the reactive sur-

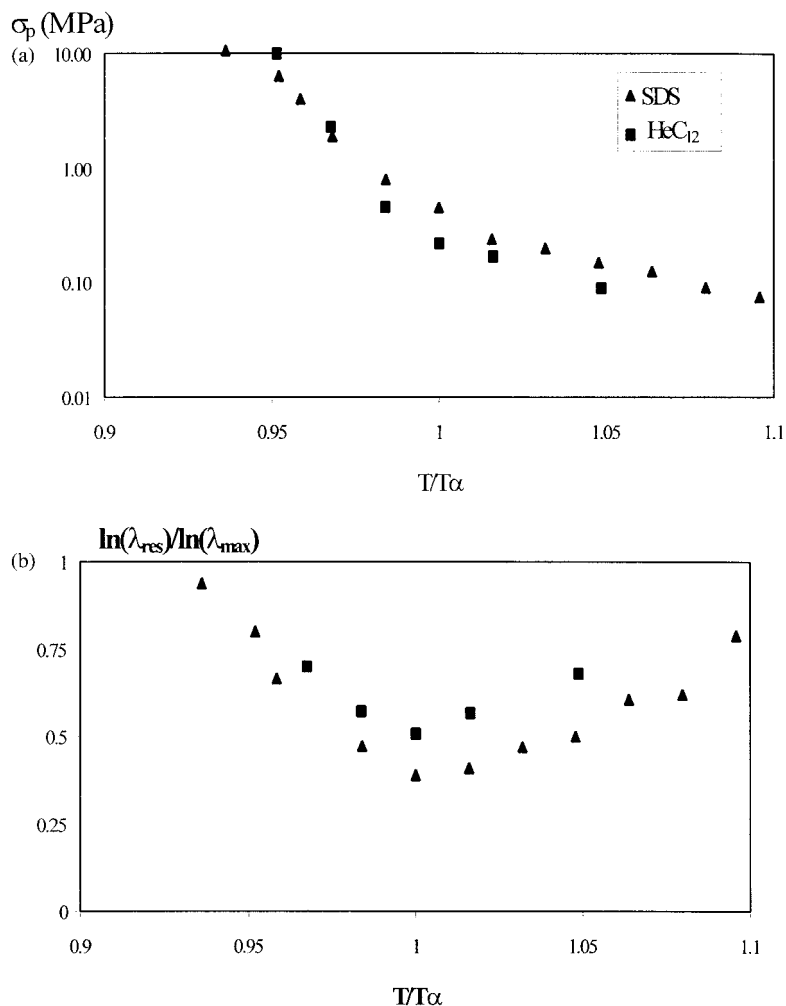


**Figure 4** (a) Evolution of the plastic flow stress ( $\sigma_p$ , log scale) versus temperature for two latex films from the OS-series. Triangles: SDS; squares: HeC<sub>12</sub>. (b) Evolution of the normalized residual deformation  $[\ln(\lambda_{res})/\ln(\lambda_{max})]$  versus temperature for two latex films from the OS-series. Triangles: SDS; squares: HeC<sub>12</sub>.

factant films. Considering the reduced scale ( $T/T_\alpha$ ), the differences between both samples are lower than the measurement precision limits. Thus, there is practically no difference in the studied thermomechanical behavior of the films due to the grafting of the surfactant at the surface of the latex particles or in the particle interior. However, this only applies to the properties of dry films, as will become clear in the following section.

#### *Effect of Water on the Film Properties*

After full formation, the films are immersed into water and periodically weighed to follow the kinetics of water uptake. Figure 5 shows kinetics related to the three samples of the OS-series. A great difference between the samples with SDS

and the samples with surfmers is observed: after being treated 1 month, SDS samples contain more than 140% of their initial weight of water, whereas in the same conditions the water contents of HeC<sub>12</sub> and C<sub>12</sub>MPOE are 3 and 8%, respectively. It may be noted that, as the non-grafted surfactant was eliminated by washing in the HeC<sub>12</sub> and C<sub>12</sub>MPOE latices, the total amount of hydrophilic moieties in the films are reduced compared to the SDS one.

To compare the mechanical properties of dry and hydrated films, we performed tensile tests until break of the sample (at 24°C and 50 mm min<sup>-1</sup>). The experiments were performed on three samples for each state (dry and hydrated). Although the stress–strain curves were reproduc-

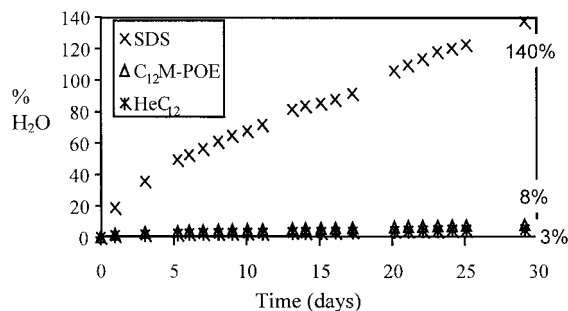


**Figure 5** Water uptake kinetics for latices, as a function of surfactant type (conventional or reactive) for the OS-series.

ible for stretching ratios  $\lambda$  smaller than 6 (regarding the precision limits of the measurements), the number of samples was not large enough to perform a good statistical analysis of the deformation at rupture. It is therefore not our purpose to discuss this parameter in a quantitative manner.

By comparing a dry and a 30% hydrated film, in the case of SDS-based latex, a decrease of both the plastic flow stress ( $\sigma_p$ ) and the strain to failure ( $\epsilon_r$ ) are observed (Fig. 6).  $\sigma_p$  decreases from 6.5 MPa in the case of the dry film to 2 MPa for the wet film with 30% of water; at the same time,  $\epsilon_r$  slightly decreases from 3.75 to 3.35. In addition, we investigated the drying process of the 30% hydrated SDS film in the conditions of film formation process (i.e., at 32°C and 75% RH). We found a continuous increase of  $\sigma_p$  (from 2 to 6.5 MPa) versus water content (from 30% to 0) as illustrated in Figure 7.

Although the HeC<sub>12</sub> and C<sub>12</sub>MPOE films can be only weakly hydrated, the mechanical properties of these films are also quite modified by the presence of water molecules (Fig. 8): a sharp decrease of the yield stress is observed, but this time combined with an increase of the strain to failure:  $\epsilon_r$  increases from 5 to 6.8.

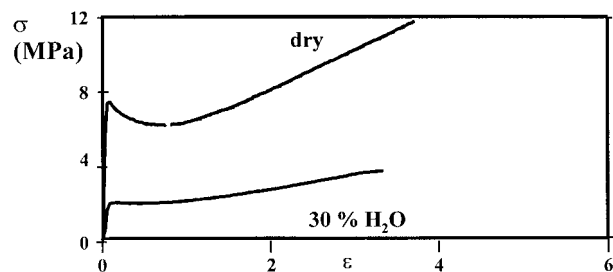


**Figure 6** Influence of water on the stress versus strain behavior for the SDS sample at 24°C and 50 mm min<sup>-1</sup> (conventional surfactant, OS-series).

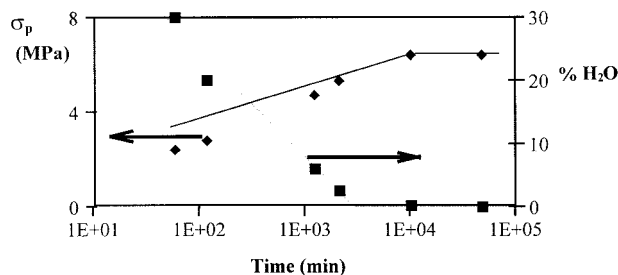


**Figure 7** Evolution of the plastic flow stress ( $\sigma_p$ , diamonds) and the water content (squares) upon drying time for the SDS sample (conventional surfactant – OS-series).

In conclusion, for both conventional and reactive surfactant-based latices, the hydration of the films leads to a decrease of the plastic flow stress. It may be noticed that, although the drop of  $\sigma_p$  is comparable for samples containing either conventional or reactive surfactants (Figs. 5 and 7), the amounts of water responsible for this decrease are really different. Thus, the implied mechanisms are without any doubt different. They will be investigated in the following section.

### One-Step Semicontinuous Systems (MJ-Series)

#### Mechanical Behaviors of Dry Films

The tensile behavior of the films cast from the MJ-latices has also been investigated versus temperature. The evolutions of plastic flow stress and residual deformation versus temperature for the MJ-latex films are reported in Figure 9(a,b), respectively. The general shapes of both curves are similar to the ones for the OS-series. The plastic flow stress decreases when temperature increases, whereas the normalized residual strain displays a minimum value, indicating the compe-

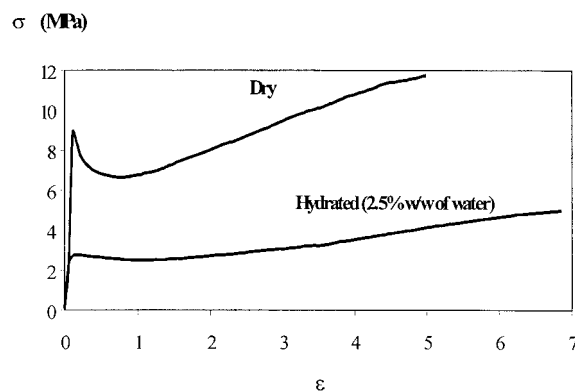


**Figure 8** Influence of water on the stress versus strain behavior at 24°C and 50 mm min<sup>-1</sup> for the HeC<sub>12</sub> sample (reactive surfactant HeC<sub>12</sub>, OS-series).

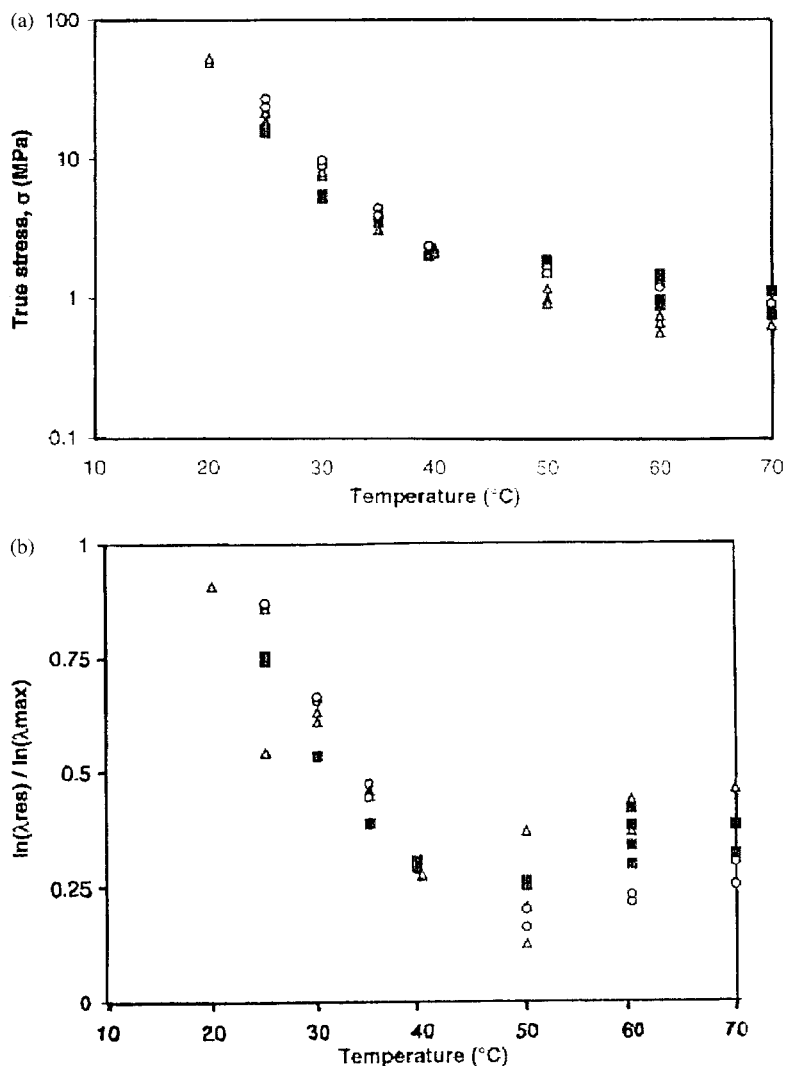


**Figure 9** (a) Evolution of the plastic flow stress ( $\sigma_D$ , log scale) versus temperature for the latex films from the MJ-series. (b) Evolution of the normalized residual deformation  $[\ln(\lambda_{res})/\ln(\lambda_{max})]$  versus temperature for the latex films from the MJ-series. Squares: 55SDS; circles: 55M141; triangles: 55CRO.

tition between rubberlike and flow behavior of the polymer. When we compare the results from the point of view of conventional and reactive surfactants, the conclusions drawn from the OS-series are confirmed by the results obtained for the MJ-series of latices (55SDS, 55M141, and 55CRO).

#### Mechanical Behavior of Wet Films

Concerning the water uptake process, the decrease of the water uptake in the case of films prepared with reactive surfactants is not observed. Actually, the differences in the amount of water uptake for the MJ-latices are rather limited: after 2 weeks, the amount of water in

55SDS, 55M141, and 55CRO are, respectively, 26, 28, and 34%. The fact that the MJ-films take up similar amounts of water can be attributed to the fact that the nongrafted surfmer has not been removed in the 55M141 and 55CRO latices before the films were cast. Considering the tensile behavior of dry and hydrated films, it appears once again that the plastic flow stress is lowered when some water is present inside the film. Nevertheless, this decrease appears to be rather limited: for example, for the 55M141 films, the plastic flow stresses are 2 (hydrated state) and 2.4 MPa (dry state), whereas the strain at rupture is 7.9 (hydrated state) and 6.4 (dry state), respectively (Fig. 10).



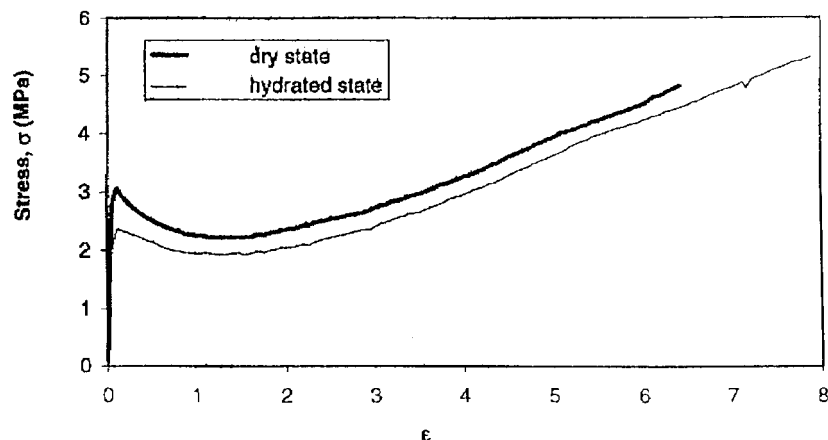


**Figure 10** Influence of water on the stress versus strain behavior for the 55M141 sample (reactive surfactant with a maleate function, MJ-series).

Finally, it can be concluded that the lowering of the stresses has been observed for all the films, whether they contained polymerizable or conventional surfactants, and for both sets of lattice (MJ and OS). To explain this decrease, two different mechanisms can be proposed. When water molecules are localized in voids of nano- or microsize inside the film, the sample can be regarded as a composite with two distinct phases: polymer and water. The decrease of the stresses has therefore a mechanical origin. In the presence of these aggregates, the film becomes heterogeneous and consequently less transparent (due to light scattering). On the other hand, water molecules can also be present inside the bulk of the polymer. When the macromolecules display polar groups, strong interactions between water molecules and those polar groups can take place. Thus, macromolecule/water interactions lead to a plasticization phenomenon that goes with a decrease of the glass transition of the film. As the tensile properties of the films were measured at a constant temperature (20°C, close to  $T_g$  of the dry film), the decrease of the stress may in this case have a physical, molecular origin.

To elucidate which of these mechanisms play a main role, we performed calorimetric and dynamic mechanical analysis on hydrated and dry samples.

#### Localization of Water Molecules in the Films

To check the plasticization of polymers by water molecules, DSC experiments have been carried out to detect a shift of the glass transition temperature.  $T_{g1}$  and  $T_{g4}$ , respectively, and the onset and the offset temperature (at which the meta-

stable state is reached), are reported in Table II for the OS-series. Two different results are obtained, depending upon the nature of the surfactant. In the case of classical surfactant (SDS), no shift of  $T_g$  is measured:  $T_{g1}$  and  $T_{g4}$  are identical, even when the amount of water is 30%. Similar results have also been observed in the case of the 55SDS sample. Moreover, the main  $\alpha$ -relaxation temperature of the copolymer prepared with SDS, as studied by dynamic mechanical experiments, also remains constant.

Figure 11 shows the evolutions of the modulus and the loss factor versus temperature for the SDS film. When the hydrated film is cooled down, the modulus increases sharply in two steps at, respectively,  $-10$  and  $-35^\circ\text{C}$ , while at the same time the loss factor goes through two distinct maxima. When heating, the modulus drops sharply again at a temperature around  $-10^\circ\text{C}$ , and  $\tan \phi$  displays one single broad peak (for  $-40^\circ\text{C} < T < 10^\circ\text{C}$ ). Because this behavior is not

**Table II** Influence of Water on the Glass Transition Temperature and the Main Mechanical Relaxation Temperature ( $T_\alpha$ ) for the OS Lattices

	$T_{g1}$ (°C)	$T_{g4}$ (°C)	$T_\alpha$ (1 Hz) (°C)
SDS dry	14	24	40
SDS hydrated (30%)	14	24	40
HeC <sub>12</sub> dry	13	25	37
HeC <sub>12</sub> hydrated (3%)	12	25	33
C <sub>12</sub> MPOE dry	13	26	35
C <sub>12</sub> MPOE hydrated (8%)	11.5	27	32

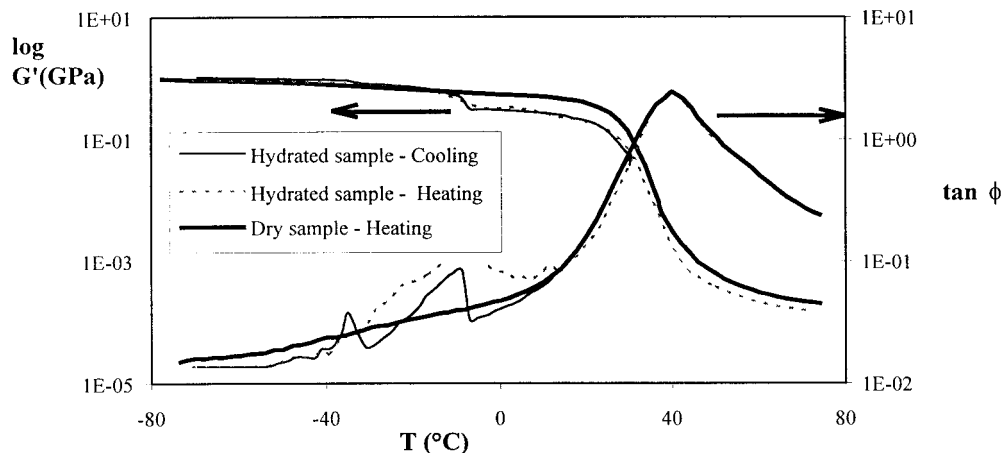


**Figure 11** Isochronal dynamic mechanical spectra of the SDS films (hydrated and dry states). Solid line: hydrated films during cooling from 25 to  $-70^{\circ}\text{C}$ ; dotted line: hydrated films during subsequent heating from  $-70$  to  $50^{\circ}\text{C}$ ; thick solid line: dry film during heating from  $-70$  to  $70^{\circ}\text{C}$ .

observed for the dry film, it can be clearly attributed to the crystallization/melting of water. This result has been confirmed by DSC, where two endothermic crystallization peaks were observed in the same temperature range when cooling a hydrated sample. Then, during thawing, the (water) crystallites' melting occurs at temperatures slightly higher than  $0^{\circ}\text{C}$ . These observations were also confirmed by wide-angle X-ray scattering measurements. It can be concluded that, in the case of conventional surfactant-based films, the water forms a second phase in the polymer, but does not interact directly with the macromolecules (no plasticizing effect). Some authors have shown that during the film formation process, the surfactant molecules can migrate to form domains at the surface and in the film.<sup>11,12</sup> These

highly hydrophilic domains are able to trap a large amount of water when the film is hydrated, without any plasticizing effect.

In contrast, a water plasticization phenomenon is detected for samples containing grafted reactive surfactant: in the case of the OS-series, both  $T_{g1}$  and  $T_{g4}$  (measured by DSC) of HeC<sub>12</sub> and C<sub>12</sub>MPOE films are lowered; however, the variations are small. This plasticization appears more visibly through dynamic mechanical experiments. Figure 12 presents the results concerning the HeC<sub>12</sub> latex. Similar results have been observed also for the films with the others surfmers (55M141, 55CRO, and C<sub>12</sub>MPOE). The vertical arrows in Figure 12 point to the maximum in the main relaxation peaks and highlight a difference of  $4^{\circ}\text{C}$  between the peaks. Moreover, the shape of

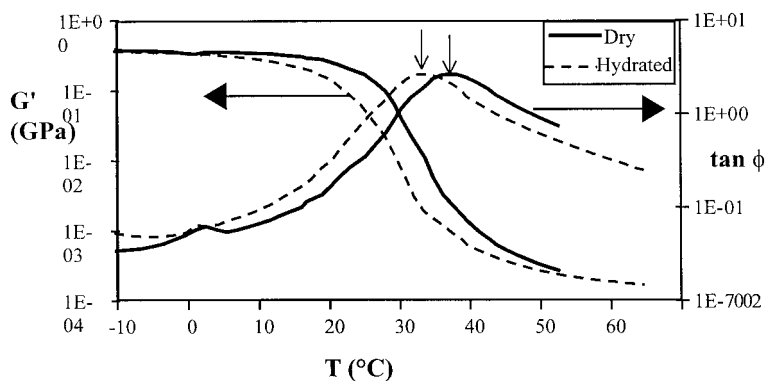


**Figure 12** Isochronal dynamic mechanical spectra measured at 1 Hz: effect of water (reactive surfactant HeC<sub>12</sub>). Solid line: 30% hydrated films during heating from  $-10$  to  $70^{\circ}\text{C}$ ; dotted line: dry film during heating from  $-10$  to  $50^{\circ}\text{C}$ .

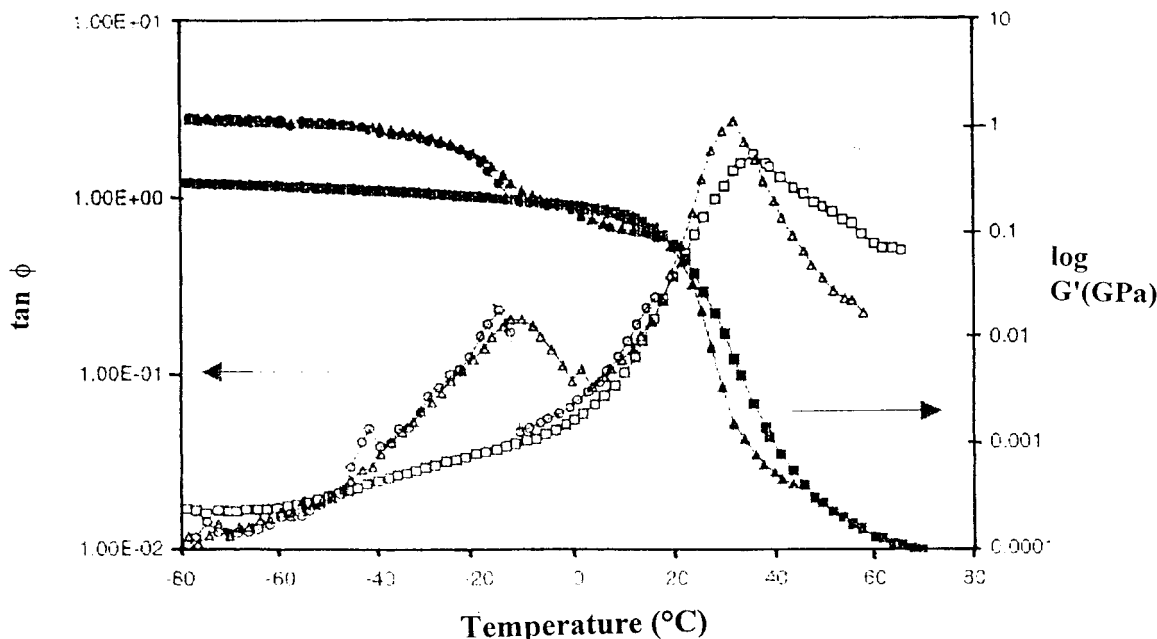


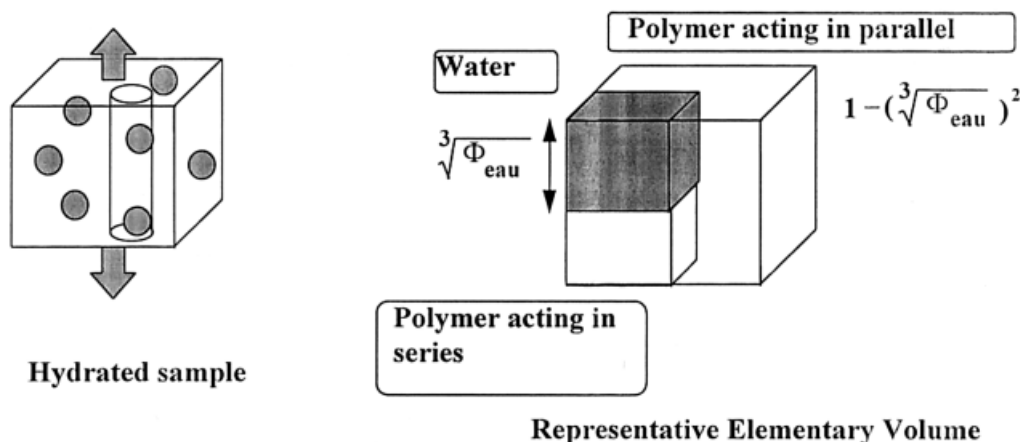
**Figure 13** Isochronal dynamic mechanical spectra measured at 1 Hz: effect of water (reactive surfactant 55M141). Circles: hydrated films during cooling from 25 to  $-70^{\circ}\text{C}$ . Triangles: hydrated films during subsequent heating from  $-70$  to  $50^{\circ}\text{C}$ . Squares: dry film during heating. Filled and open symbols correspond to the evolution of the modulus  $G'$  and the loss factor, respectively.

the loss factor curves and of the modulus drop in the temperature range  $20^{\circ}\text{C} < T < 60^{\circ}\text{C}$  is also affected. Because the surfactant is grafted to the surface of the particles or incorporated in polymer chains in the particle interior,<sup>8</sup> it cannot segregate during the film formation process and is embedded inside the film. This results in the presence of hydrophilic sulfonate groups in the macromolecules. When the film is rehydrated, the water molecules will go preferentially near these sites, and the plasticization may occur.

In the case of OS-latexes, when the nongrafted surfactant was removed from the latex, neither DSC experiments nor dynamic mechanical analysis revealed the presence of free water, leading to water crystallization or ice melting. In contrast, in the case of the MJ-series, the shift of  $T_{\alpha}$  associated to the plasticization is accompanied by a large composite effect, evidenced by the presence of the  $\tan \delta$  peaks at temperatures below  $0^{\circ}\text{C}$  (Fig. 13). Because the grafting reaction of the surfmer for these latexes (55M141 and 55CRO) was not complete<sup>8</sup> and because the latexes were not purified before the films were cast, the presence of the additional peaks must reflect the presence of the nongrafted surfactant molecules. In this case, the fraction of the surfmer that has reacted and is present at the particle surface or

buried in the particle interior is localized, after casting, throughout the bulk of the film in a relatively homogeneous way and leads to plasticization. The fraction that has not reacted and is not grafted gives rise to a composite (polymer/water) film, just as in the nonreactive surfactant-based latex.

As the mechanisms ruling the influence of the water molecules in the films have been elucidated, we can now reconsider the results of the mechanical tests of dry and hydrated films. As these experiments were performed in the glass transition temperature zone, a small variation of the molecular mobility induced by plasticization can lead to a sharp variation of the mechanical properties. As expected, this plasticization leads to a decrease of the yield stress and to an increase of the elongation at break (Fig. 8). In the case of films synthesized in the presence of conventional surfactants, the water is concentrated in some domains containing variable concentrations of surfactant and/or poly(acrylic acid), so that these zones can crystallize at different temperatures. The mechanical properties of the films are then modified, through a composite effect; the material, in such a case, consists of polymeric matrix and water inclusions. This results in a decrease of the plastic stress. Moreover, the high dispersion



**Scheme 1** Series-parallel model representative of the hydrated sample.

of the strain at rupture ( $\epsilon_r$ ) is also consistent with the fact that the films are very heterogeneous when they contain a large amount of water (Fig. 7). In the next section, we will consider each mechanism in a quantitative way to calculate the decrease of the plastic flow stress.

### Quantitative Analysis of the Decrease of the Plastic Flow Stress

#### Calculations Based on a Mechanical Coupling Approach

When the decrease of the stress has a mechanical origin, it can be qualitatively described with a mechanical coupling model. From a very general point of view, the elastic modulus of a filled polymer is affected by the elastic properties of its constitutive phases (i.e., modulus and Poisson ratio), the volume fraction of filler, and the morphology (i.e., shape, aspect ratio, dispersion, and interactions between fillers). Various models are proposed in the literature to understand the complex interplay between these parameters and to give a prediction of the elastic modulus of polymer composites. Among the different approaches, one set of theoretical predictions is based on phenomenological approaches (e.g., series-parallel model of Takayanagi<sup>13</sup>) that can be very useful as a first step to estimate roughly the effect of the mechanical coupling in a biphasic system (mechanical coupling means how energy of deformation is distributed between the distinct phases). In this work use was made of a series-parallel equation to estimate the plastic stress, taking into account the volume fraction of water in the film ( $\Phi_{\text{water}}$ ), as illustrated in Scheme 1.

In such a representation, the behavior of the material is directly related to the fraction of polymer acting in parallel, as the contribution of water to the mechanical resistance is negligible. It can be deduced from geometrical considerations that the relationship between the plastic flow stress of the composite film and the volume fraction of water is given by:

$$(\sigma_p)_{\text{Composite}} = (\sigma_p)_{\text{Polymer}} [1 - (\sqrt[3]{\Phi_{\text{eau}}})^2] \quad (1)$$

The values of plastic stress obtained with eq. (1) compare well with the evolution of the experimental data in the case of the SDS sample (see full line in Fig. 7). Of course, this simplified approach does not take into account the localization of the water into the film that leads to an underestimation of the decrease at a low value of water volume fraction. Moreover, it assumes implicitly that the pressure inside the water is negligible. This is, however, a second-order assumption regarding the difference of mechanical behavior between polymer and water, and the size of water inclusion is large enough to give a diffraction pattern. Thus, the model only provides a rough estimation of the decrease of the plastic flow stress with the water content within the composite.

#### Calculations in the Frame of the qpd Model

In recent years, a theory of nonelastic deformation of polymers based upon molecular mobility concepts has been developed in the G.E.M.P.P.M. This theory, already described in other references,<sup>14,15,16</sup> has been improved by including unloading behavior and strain hardening. The main as-

sumptions are as follows: (1) the existence of quasi point defects (qpd) corresponding to nanofluctuations of specific volume; (2) the hierarchically constrained nature of molecular dynamics; and (3) under the application of a stress, the nucleation and growth of local shear microdomains (smd) (carriers of the anelastic strain) until they ultimately merge irreversibly with one another (viscoplastic strain).

Previously, molecular mobility in polymers was analyzed in terms of hierarchically correlated movements,<sup>14</sup> leading to an expression of the mean molecular mobility time  $\tau_{\text{mol}}$ :

$$\tau_{\text{mol}} = t_0 \left( \frac{\tau_\beta}{t_0} \right)^{1/\chi} \quad (2)$$

In this expression,  $\tau_{\text{mol}}$  corresponds to the time necessary for a structural unit to move on a distance equivalent to its length.  $\chi$  ( $0 < \chi < 1$ ) is a correlation parameter related to the degree of disorder. Hence,  $\chi = 0$  corresponds to a fully constrained situation and  $\chi = 1$  is a constraint-free situation (perfect crystal and perfect gas, respectively). Thus, it appears that  $\chi$  is constant ( $=\chi(T_g)$ ) when the microstructure is frozen ( $T < T_g$ ) and increases in the metastable equilibrium ( $T > T_g$ ). A Taylor expansion has been used to describe such an evolution:  $\chi_0 = \chi(T_g) + a(T - T_g)$ , where  $a$  is a constant,  $t_0$  is a scaling parameter, and  $\tau_\beta$  is the time of the preliminary movement (taken as the  $\beta$  secondary process). Thermomechanical activation of this relaxation yields:

$$\tau_\beta(\sigma) = \tau_{\beta 0} \exp \left[ \frac{U_\beta}{kT} \left( 1 - \frac{\sigma}{\sigma_0} \right)^{3/2} \right] \quad (3)$$

where  $\sigma_0$  is the limit of the yield stress necessary for overpassing conformational change when the temperature becomes 0 K [i.e.,  $\sigma_0 \approx G_0/2\pi$  (Frenkel argument)].

The anelastic times (related to the nucleation and expansion of smd) are distributed in between the elementary time  $\tau_\beta(\sigma)$  and  $\tau_{\text{mol}}(\sigma)$ . On the other hand, the viscoplastic times (corresponding to the motion of structural units over large distances) are distributed around  $\tau_{\text{mol}}(\sigma)$ , because the disorder is spatially distributed in the material (in practice, we have chosen to incorporate the disorder's characteristic through a Gaussian distribution of the correlation parameter, which results in a log-normal distribution of the characteristic times). These main ideas lead to a macroscopic compliance  $J = \epsilon/\sigma$  written as the sum of

the elastic, the anelastic, and the viscoelastic components:

$$J_\alpha(t) = J_u + J_{an_\alpha} \times \left[ 1 - \exp \left( - \left( \frac{t}{\tau_{rm}} \right)^\chi \right) \right] + J_{vp_\alpha} \left( \frac{t}{\tau_{rm} J_r / J_{an}} \right)^{\chi'} \quad (4)$$

with

$$\tau_{rm} = \chi^{1/\chi} \tau_{\text{mol}} \quad \text{and} \quad J_{vp_\alpha} = J_r - J_u - J_{an_\alpha} \quad (5)$$

where  $J_u = 1/G_u$  is the unrelaxed compliance associated with the  $\alpha$ -relaxation and  $J_r = 1/G_r$  is the rubber shear compliance.  $J_{an_\alpha}$  and  $J_{vp_\alpha}$  are, respectively, the intensity of anelastic and viscoplastic processes.  $\chi'$  ( $0 < \chi < \chi' \leq 1$ ) accounts for the spatial distribution of entanglements (for example,  $\chi' = 1$  for glasses).<sup>17</sup> On this basis, an incremental calculation allows us to determine the contribution (anelastic and viscoplastic) of each population to the macroscopic deformation. The procedure to determine the set of parameters is fully documented in ref. 17 (see Table III).

When stress is applied, the nucleation and growth of smd correspond to an increase of the disorder and then an increase of  $\chi$  with  $\epsilon_{an}$ . Moreover, macromolecular orientation occurs and leads to<sup>18</sup>: (1) a decrease of molecular mobility due to a better organization of the material occurring with the development of viscoplastic strain (introducing chain orientation). This should result in a decrease of  $\chi$ ; (2) entropic processes: at high temperature, the polymer is in the rubbery state, which involves purely entropic effects. The description of rubberlike elasticity was first developed by considering an ideal network, constituted of freely jointed segments.<sup>19</sup> Recently, refinements were introduced to take into account finite elongation of the chains.<sup>20</sup> As we describe

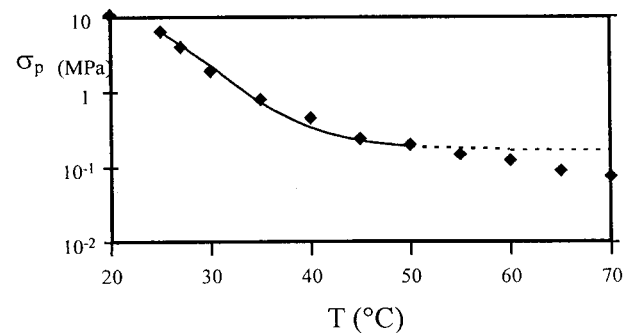


**Figure 14** Comparison between experimental (squares) and simulated (line)  $\sigma_p$  versus temperature.

**Table III Values of the Parameters from the qpd Model**

$T_g$ (°C) (measured by DSC)	14
$\chi(T_g)$	0.255
$U_\beta$ (J mol <sup>-1</sup> )	51387
$\tau_{0\beta}$ (S)	$2.6 \times 10^{-16}$
$t_0$ (S)	$2 \times 10^{-10}$
$a$	0.006
$G_u$ (Pa)	$8.4 \times 10^8$
$G_r$ (Pa)	$0.5 \times 10^6$

the entropic effect on the basis of ref. <sup>20</sup>, we propose to relate the decrease of  $\chi$  with the change of chains entropy (i.e., through an inverse Langevin function).

Computer-simulated  $\sigma$ - $\epsilon$  curves for loading and unloading regimes have shown fairly good accordance with experiments for broad ranges of  $T_{\text{def}}$ ,  $\epsilon_{\text{def}}$ , and  $\dot{\epsilon}_{\text{def}}$  with one set of parameters. The experimental and simulated data concerning the evolution of  $\sigma_p$  as a function of temperature are reported in Figure 14. Good agreement is observed up to 50°C. However, in the high-temperature range, a small deviation appears that can be related to the flow of macromolecules, which is not introduced in the calculations.

Next, the qpd model is used as a predictive tool to quantify the expected decrease of plastic stress with the amount of humidity in the film. To perform the calculations when the polymer is in the wet state, we changed the value of the glass transition in agreement with the experimental decrease of  $T_g$  (Table II). For example, in the case of HeC<sub>12</sub>, taking into account the shift of  $T_g$  (decrease of 4°C), the stress-strain curve at  $T = 20^\circ\text{C}$  is recalculated and leads to a decrease of the plastic flow stress value by a factor of 3. This decrease is consistent with the experimental data.

## CONCLUSION

It has been shown that the presence of grafted reactive surfactant molecules in some latices does not affect the thermomechanical properties of dry films over a large temperature range from below to well above the glass transition temperature. This means that one can use reactive surfactants (surfmer) for other reasons (for example, to increase colloidal stability of the latex) without affecting the dry film proper-

ties. We have highlighted that the behavior of the films is largely sensitive to the presence of water molecules. In that case, two distinct phenomena can be observed. In the case of reactive surfactant-based films, a plasticization effect is measured and attributed to the presence of the grafted surfactant molecules inside the film. These molecules introduced hydrophilic moieties that are dispersed inside the polymer in a more or less homogeneous way. This plasticization effect is not observed in the conventional surfactant-based films. Another effect is the formation of a composite material (water/polymer), which is also observed in the case of reactive surfactant, when the nonreacted molecules are not removed from the material. It is then attributed to the presence of ungrafted surfactant molecules (either reactive or conventional), which segregate during the film formation and create highly hydrophilic domains that may trap water molecules. This last point underlines the importance of synthesizing latices containing mainly grafted surfactant instead of a mix of grafted and adsorbed surfactant to improve the film resistance to water molecules' uptake.

The authors gratefully thank Rhodia Recherches (Aubervilliers, France) for the financial support accorded to this project through the Ph.D. fellowship of O. Sindt.

## REFERENCES

- Asua, J. M.; Schoonbrood, H. A. S. *Acta Polym* 1999, 49, 671.
- Holmberg, K. *Prog Org Coat* 1992, 20, 235.
- Guyot, A.; Tauer, K. *Adv Polym Sci* 1994, 111, 43.
- Tauer, K. *Polym News* 1995, 20, 342.
- Guyot, A. *Curr Opin Colloid Interface Sci* 1996, 1, 580.
- Nagai, K. *Trends Polym Sci* 1996, 4, 122.
- Tauer, K. in *Polymeric Dispersions: Principles and Applications*; Asua, J. M., Ed.; Kluwer Academic Publishers: Dordrecht, 1997.
- Sindt, O.; Gauthier, C.; Hamaide, T.; Guyot, A. *J Appl Polym Sci* 2000, 77, 2768-2776.
- Schoonbrood, H. A. S.; Unzue, M. J.; Beck, O. J.; Asua, J. M.; Montoay Goni, A.; Sherrington, D. C. *Macromolecules* 1997, 30, 6024.
- Etienne, S.; Cavallé, J. Y.; Perez, J. *Rev Sci Instrum* 1992, 53-8, 1261.
- Zhao, C. L.; Holl, Y.; Pith, T.; Lambla, M. *Colloid Polym Sci* 1987, 265, 823.
- Juhué, D.; Wang, Y.; Lang, J.; Leung, O. M.; Goh, M. C.; Winnick, A. M. *J Polym Sci, Part B: Polym Phys* 1995, 33, 1123.

13. Takayanagi, M.; Uemura, S.; Minami, S. *J Polym Sci, Part C: Polym Lett* 1964, 5, 113–122.
14. Perez, J. *Physics and Mechanics of Amorphous Polymers*; Balkem, A. A., Ed.; Rotterdam: Brookfield, 1998.
15. Perez, J.; Ladouce, L.; Quinson, R. *Deformation, Yield, and Fracture of Polymers*; Institute of Materials: London, Proceedings 1994, 25/1–25/4.
16. Gauthier, C.; David, L.; Ladouce, L.; Quinson, R.; Perez, J.; *J Appl Polym Sci* 1997, 65, 2517–2528.
17. Chabert, E.; Ershad Langroudi, A.; Gauthier, C.; Perez, J. *Plast, Rubbers Compos* 2001, 30 (2), 56–67.
18. Sindt, O.; Gauthier, C.; Perez, J. *Proceedings of Deformation, Yield, and Fracture of Polymers*; Cambridge Univ. Press: Cambridge, 1997, 238–241.
19. Mark, J. E. *Physical Properties of Polymers*; ACS Professional Reference Book: Washington, DC, 1993.
20. Arruda, E. M.; Boyce, M. C. *J Mech Phys Solids* 1993, 41, 389–412. 0